Electrooxidation of H_2, CO, and H_2/CO Mixtures on a Well-Characterized $Pt_{70}Mo_{30}$ Bulk Alloy Electrode

B. N. Grgur, N. M. Markovic, and P. N. Ross, Jr.*

Materials Sciences Division, Lawrence Berkeley National Laboratory, University of California, Berkeley, California 94720

Received: August 19, 1997; In Final Form: February 5, 1998

The electrochemical oxidation of hydrogen (H_2), carbon monoxide (CO), and their mixtures (500 ppm−2%) on a well-characterized $Pt_{70}Mo_{30}$ bulk alloy was examined using the rotating disk electrode technique in 0.5 M H_2SO_4 at 333 K. The electrodes were transferred to and from a UHV chamber, where surface analyses were conducted using a combination of low-energy ion scattering (LEIS), Auger electron spectroscopy (AES), and X-ray photoelectron spectroscopy (XPS). The surface composition of this alloy after sputter-etching and annealing in UHV was slightly enriched in Pt to a composition of $Pt_{77}Mo_{23}$. The kinetics of H_2 oxidation are not measurably affected by the presence of the Mo in the surface. The shapes of the polarization curves for the oxidation of the H_2/CO mixtures are qualitatively similar to those for the $Pt_{50}Ru_{50}$ alloy examined previously: a high current−potential slope (ca. 0.5 V/dec) at low overpotential followed by a transition to a highly active state where the current approaches the diffusion-limiting current; the potential where the transition to the active state occurs decreases with decreasing CO concentration and decreases with increasing temperature; the current in the low-overpotential region is roughly inverse half-order in the CO partial pressure. The current densities in the low-overpotential region are comparable to those on $Pt_{50}Ru_{50}$ alloy and about a factor of 50 times those on a pure Pt surface. While the anodic stripping of irreversibly adsorbed CO is very different from that on the $Pt_{50}Ru_{50}$ alloy, with most of the CO_{ads} being oxidized only above 0.6 V (RHE), there is direct evidence for the oxidation of small amounts of CO_{ads} in the low-overpotential region of 0.05−0.5 V. The mechanism of action of Mo in the Pt surface in enhancing H_2 oxidation in the presence of CO thus appears to be very similar to that of Ru: a reduction in the steady-state coverage of CO_{ads} on the Pt sites by oxidative removal, freeing Pt sites for H_2 oxidation.

1. Introduction

A major problem in the development of low-temperature fuel cells for transportation applications is the deactivation of the Pt anode catalyst by even trace levels, e.g., 10−100 ppm, of carbon monoxide (CO). The anode deactivation produced by low concentrations of CO necessitates the use of either pure hydrogen or an extensive purification system for hydrogen generated on board the vehicle by steam reforming a carbonaceous fuel. A review of efforts to develop alternative catalysts that are tolerant to CO in hydrogen can be found in ref 1.

In previous studies,[2−4] we investigated the oxidation of H_2, CO, and their mixtures on Pt, Ru, Pt−Ru alloys,[2,3] and Pt_3-Sn,[1,4] all as solid electrodes pretreated and characterized in UHV and transferred into a rotating disk electrode assembly for kinetic evaluation of the reaction rates. In a recent Letter,[5] we reported the first results for the electrooxidation of H_2 and H_2/CO mixtures on a solid solution $Pt_{75}Mo_{23}$ alloy using identical methodology. The characteristics of the $Pt_{75}Mo_{25}$ surface for the oxidation of H_2/CO mixtures were found to be remarkably similar to those of the $Pt_{50}Ru_{50}$ alloy. This result is surprising and interesting in view of the seemingly disparate chemistry of Ru and Mo. In the present, we report a full study on the electrochemistry of the Pt−Mo (30 at. % Mo) bulk alloy in acidic solution, the stability of Mo in the alloy surface, the nature of CO_{ads} on the alloy surface, and the role of CO_{ads} on the kinetics the oxidation of dissolved CO gas and H_2/CO gas mixtures containing from 500 ppm to 2% CO.

2. Experimental Section

The polycrystalline Pt−Mo alloy was prepared as a boule by arc-melting of the pure elements in an argon atmosphere and a homogenizing heat treatment. Details of the preparation procedure, which was the same as used for Pt−Ru alloys, are given in ref 2. The nominal composition of the alloy from the weights of the pure metals was 25.0 at. % Mo; however, elemental analysis (by atomic absorption) of the arc-melted boule indicated a composition of 30.3% Mo. X-ray diffraction analysis confirmed the formation of a single-phase fcc structure with lattice constant 0.3908 nm, in agreement with the lattice constant given for the Pt solid solution alloy with 30 ± 5 at. % Mo in Pearson.[6a] Pt loss (relative to Mo) is presumed to have occurred during arc-melting of the metals, since Pt has a much higher vapor pressure than Mo.[6b] The alloy boule was precision ground into a cylinder shape to fit into a Pine Instruments insertable rotating disk electrode (RDE) arbor.[7]

LEIS, AES, and XPS data were collected using a angle-resolving double-pass cylindrical mirror analyzer. Details of the data collection procedure were reported previously.[8] For LEIS, a 2 keV $^4He^+$ ion beam was rastered over a 3 mm × 3 mm area of the surface at an incident angle of 45°. The average scattering angle was 127° with resolution less than 1°. Calibration of the LEIS sensitivity factors and the XPS binding energies

* Corresponding author: (510) 486-5530 (fax); pnross@lbl.gov (e-mail).

S1089-5647(97)02692-8 CCC: $15.00
Published on Web 03/17/1998

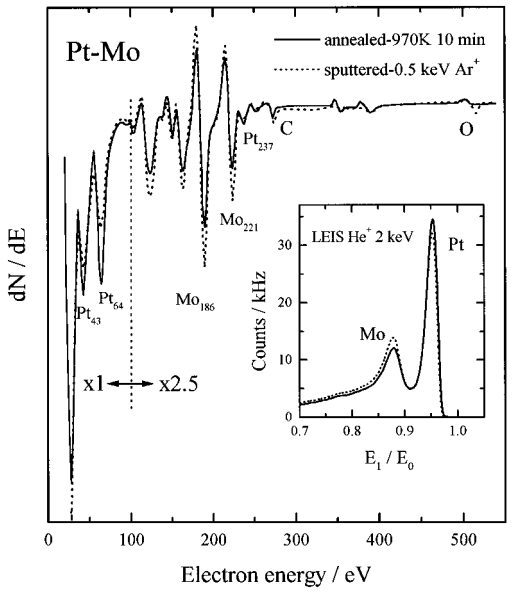

Figure 1. Derivative mode AES spectrum of the Pt−Mo alloy following sputter-cleaning (dashed curves) and annealing at 970 K (solid curves). (insert) LEIS spectra of the same surfaces.

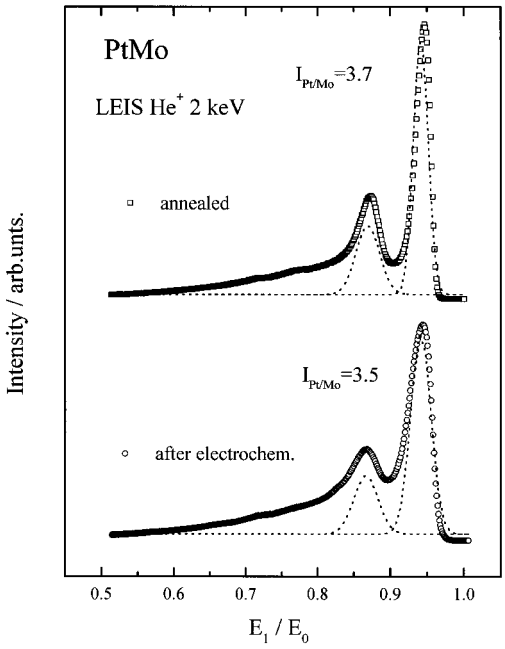

Figure 2. LEIS spectra for the Pt−Mo alloy for the clean, annealed surface and the surface following electrochemical treatment and transfer back into the UHV chamber (see text).

was carried out using pure Pt and Mo polycrystals. All XPS binding energies were referenced to the Pt $4f_{7/2}$ peak set at 71.1 eV. A conventional laboratory X-ray source was used with a Mg twin anode.

All data reported here were obtained using the alloy sample inserted into a Pine RDE arbor following cleaning and characterization in UHV. The detailed procedure for the transfer from UHV and insertion into the RDE has been given previously.[9] The procedures for measuring hydrogen oxidation current−potential curves with the Pt−Mo alloy were the same as used previously for Pt−Ru alloys, and the details are given in refs 2 and 3. All potentials given here are referred to the reversible hydrogen electrode (RHE) at the same temperature. H_2SO_4 (0.5 M) solutions were used for all electrochemical experiments.

3. Results

3.1. Surface Analyses. AES analysis was conducted primarily for the purposes of assessing surface cleanliness. A typical AES spectrum for the Pt−Mo alloy surface after numerous cycles of Ar ion sputtering (0.5 keV) and thermal annealing (973 K for 30 min) is shown in Figure 1. It did not appear practical to remove all traces of carbon and oxygen from the annealed surface; even the sputter-etched surface showed carbon and oxygen detectable by AES, and these signals are somewhat increased upon thermal annealing, probably by surface segregation from the bulk. The trace amounts remaining, however, were not considered to affect either the LEIS analysis or the electrochemical properties of the surface. The AES spectra appear to show an increase in Pt/Mo surface atomic ratio upon annealing. Typical LEIS spectra from the same surfaces are shown in the insert in Figure 1. The peak energies for Pt and Mo agreed to within ±0.5% with the values predicted by the classical equation for elastic collisions.[10] The surface composition was calculated from the peak heights, H_{Pt} and H_{Mo}, determined by fitting the spectrum with Gaussian profiles, according to

$$X_{Mo} = S_{Mo/Pt}/[S_{Mo/Pt} + (H_{Mo}/H_{Pt})_{exp}]$$

where $S_{Mo/Pt}$ is the empirical sensitivity for Mo relative to Pt. The empirical sensitivity factor was determined from the peak heights in the pure samples according to[11]

$$S_{Mo/Pt} = (H_{Mo}/H_{Pt})_{pure}(a_{Pt}/a_{Mo})^2$$

where a_{Pt} and a_{Mo} are the lattice constants for the pure metals. The resulting surface composition from the spectrum in Figure 1 for the annealed surface was 23 at. % Mo, while the sputter-etched surface was 30 at. % Mo, nominally identical to the bulk. This result indicates there is some enrichment of the surface in Pt, qualitatively consistent with the predictions of thermodynamic models.[12] It is possible that the annealing of the Pt−Mo alloy at the relatively low temperature of 973 K does not produce an equilibrated surface, and it is possible that higher temperature and/or longer annealing would have produced the highly Pt-enriched surface predicted in thermodynamic models.

The stability of Mo in the surface in 0.5 M H_2SO_4 was examined by removing the electrode from the cell, washing with water, and reinserting into the UHV chamber for analysis by LEIS. Although some contamination of the surface by impurities from the transfer were obvious, e.g., traces of carbon, LEIS peaks from both Pt and Mo were observed as shown in Figure 2, and their relative intensities indicated no loss of Mo from the surface as a result of electrochemical examination, which included repeated cycling at various sweep rates from 0 to 0.8 V.

Information about the intermetallic bonding in the annealed alloy, and about the chemical state of the Mo atom in the alloy surface in solution, was obtained by XPS analyses in UHV, in the latter case, from the sample after transfer from solution as above with LEIS analyses. Binding energies for characteristic core levels for both Pt and Mo atoms in the clean, annealed alloy surface are summarized in Table 1. The chemical shifts relative to the pure metals are qualitatively similar to those in the highly exothermic Pt_3Sn and Pt_3Ti alloys,[13] indicative of charge transfer from Mo to Pt, but perhaps to a lesser extent than in Pt_3Sn or Pt_3Ti, where the bonding has a strongly ionic character with the Sn (Ti) atom in a nearly cationic (+II) state.

TABLE 1: Core-Level Binding Energies and Chemical Shifts for Clean, Annealed $Pt_{77}Mo_{23}$ Alloy

	binding energy/eV			
	$3d_{5/2}$	$3d_{3/2}$	$3p_{3/2}$	$3p_{1/2}$
Mo	227.8	231.0	394.0	411.5
$Mo_{(PtMo)}$	227.3	230.5	393.8	411.3
shift (eV)	−0.5	−0.5	−0.2	−0.2
	$4f_{7/2}$	$4f_{5/2}$	$4d_{5/2}$	$4d_{3/2}$
Pt	71.1	74.4	315.0	331.8
$Pt_{(PtMo)}$	71.4	74.7	314.8	331.6
shift (eV)	+0.3	+0.3	+0.2	+0.2

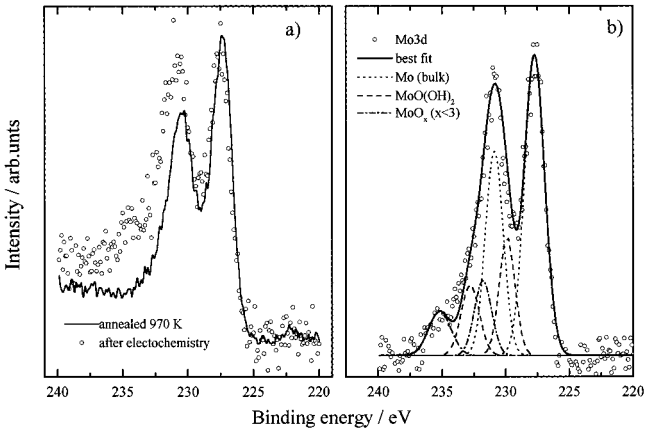

Figure 3. (a) XPS spectra from the Mo 3d core-level region for the same two surfaces shown in Figure 2. (b) Curve fitting and deconvolution (after background subtraction) of the spectrum of the electrochemically treated surface in terms of known oxidation states.

According to the calculations of Miedema,[14] the intermetallic bonding is relatively strong in Pt−Mo alloy, being intermediate between the highly exothermic alloys Pt_3Sn or Pt_3Ti and the slightly endothermic alloy Pt−Ru. Following removal of the sample from the electrochemical cell at +0.1 V, the high-resolution scan in the Mo 3d region, shown in Figure 3, shows evidence of oxidation of the Mo surface atoms upon exposure to electrolyte. The increase in intensity from 232 to 235 eV indicates a ca. +3 eV shift in the Mo $3d_{5/2}$ binding energy, which is characteristic of Mo in the +IV valence state. The spectrum from the emersed electrode strongly resembles that reported by Lu and Clayton[15] for the passive film on pure Mo, which they identified as the oxyhydroxide, $MoO(OH)_2$. The oxidation state of the Mo was independent of the potential history of the electrode or of the emersion potential (0−0.6 V). If there is electrochemical reduction of Mo to a lower valence state than +IV, this state does not survive transfer to UHV as done in this work (which was not anaerobic).

Further details of the state of Mo on the emersed electrode can be derived from the O 1s spectral region, 500−540 eV, shown in Figure 4. In this region of binding energy, one sees not only O 1s but also the Pt $4p_{3/2}$ and the Mo 3s. A pure Pt sample emersed from the cell following the same protocol as for Pt−Mo showed no measurable O 1s intensity. The adsorption of oxygen on Pt surfaces has been the subject of intensive study by XPS, and the O 1s/Pt $4p_{3/2}$ ratio as a function of coverage is well-known.[16] This calibration can be used to estimate the O/Mo stoichiometry in the present case if it is assumed that all the oxygen is bonded to Mo surface atoms. This approximation is likely to underestimate the true coverage, since if the oxygen atoms are localized on the Mo they do not screen the Pt 4p emission as much as when the oxygen is adsorbed on the Pt atoms. The O 1s/Pt 4p intensity ratio in Figure 4 is indicative of an O/Pt ratio close to unity,[16] which

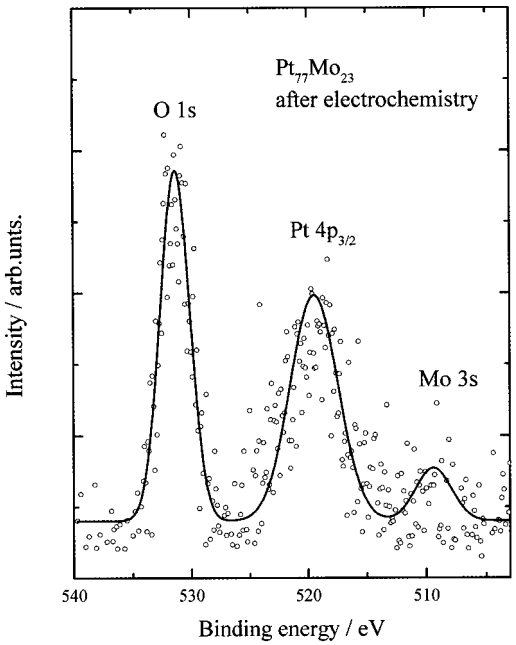

Figure 4. XPS spectra from the O 1s and Pt 4p core-level region electrochemically treated Pt−Mo alloy surface: (○) experimental data; (solid curve) best fit.

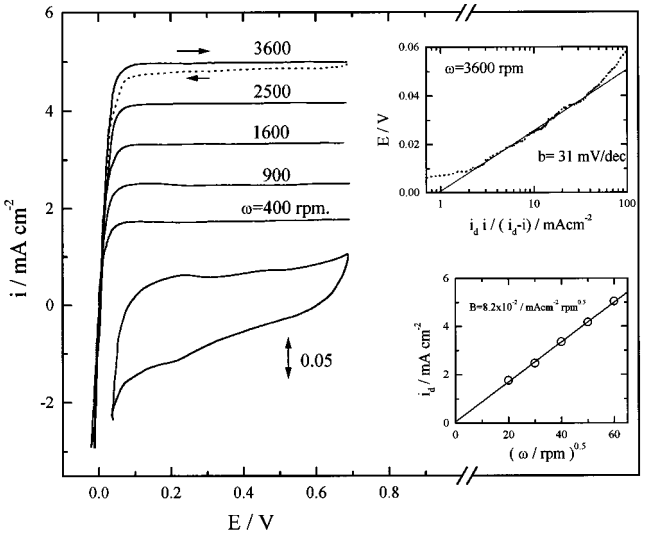

Figure 5. (lower) Cyclic voltammogram in dearated electrolyte for the $Pt_{77}Mo_{23}$ alloy surface following transfer from UHV; 50 mV s^{-1}, 0.5 M H_2SO_4 at 333 K. (upper) Current−potential curves in H_2-saturated electrolyte at 333 K; 1 mV s^{-1}. (insert, upper) Tafel plot of the current−potential curve for H_2 oxidation at 3600 rpm. (insert, lower) Levich plot of the diffusion limiting currents.

means the O/Mo stoichiometry is ca. 3/1, consistent with the identification of the state of Mo primarily as $MoO(OH)_2$.

3.2. Electrochemical Analyses. *3.2.1. Anodic Oxidation of Hydrogen.* The voltammetry of the $Pt_{77}Mo_{23}$ surface in argon-purged electrolyte and the slow sweep (1 mV/s) current−potential curve for H_2 oxidation are shown in Figure 5. Although the surface is only 23 at. % Mo, the voltammetry has very little Pt character, having no distinct peaks for hydrogen adsorption/desorption in the 0−0.3 V region, and very large pseudocapacitance in the 0.3−0.6 V region. The absence of distinct hydrogen adsorption/desorption peaks is similar to the character of the Pt_3Sn surface,[4] but the large pseudocapacitance more resembles the character of the $Pt_{50}Ru_{50}$ surface.[12] As with $Pt_{50}Ru_{50}$, the large pseudocapacitance is probably due to redox processes on the oxidized Mo surface atoms, most likely

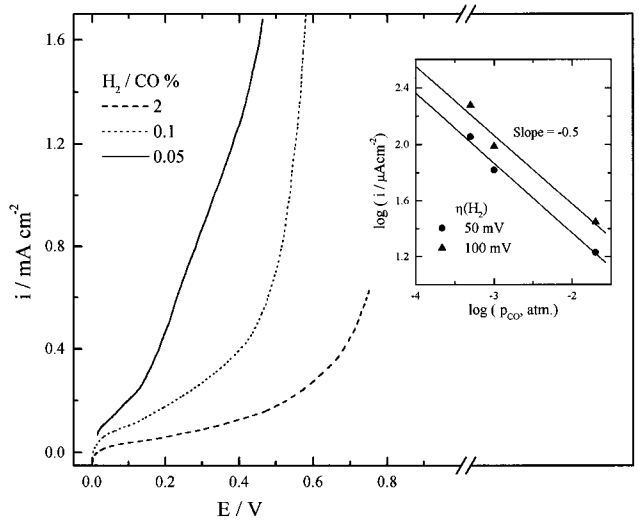

Figure 6. (left) Current−potential curve for the oxidation of H_2 on the $Pt_{77}Mo_{23}$ alloy surface containing various levels of CO at 2500 rpm; 1 mV s^{-1}, 333 K. (insert) Reaction order (in CO) plot for H_2/CO mixtures in the low potential region.

involving proton rather than oxygen transfer.[17] The voltammetry curves were unaffected by cycling in the potential region shown, the first cycle upon transfer from UHV being identical to the *n*th cycle. This is further evidence of the stability of Mo in the surface.

The kinetics of oxidation of pure H_2 on the $Pt_{77}Mo_{23}$ surface is indistinguishable from the that on the pure Pt surface.[2] The overpotential/current relation, shown in the insert, at the rotation rates used here closely follows that for pure diffusion control[2]

$$\eta = -2.3(RT/2F)\log(1 - i/i_d) \qquad (1)$$

where i_d is the measured diffusion-limited current at any rotation rate, i is the observed current density at the overpotential η, and R, T, and F have their usual meaning (at 333 K, and 2.3RT/2F is 33 mV/dec). Because the rate of reaction is so high on either the pure Pt or the Pt−Mo alloy surface relative to the rate of H_2 transport possible with the RDE, it is impossible to say whether there is a kinetic difference between the two surfaces.

3.2.2. Oxidation of H_2/CO Mixtures. The polarization curves for the oxidation of H_2 in the presence of CO (2, 0.1, and 0.05 vol %) at 333 K are shown in Figure 6. The curves are recorded on the anodic sweep (1 mV) from 0 V after switching from pure H_2 to the H_2/CO mixture and waiting for 60 min. (Quasi-steady-state currents recorded using potential steps from 0 V showed there are significant time effects for the 0.1 and 0.05 % CO gases, which we discuss below in greater detail.) As the comparison in Figure 7 for 0.1 % CO clearly shows, the shapes of these polarization curves at 1 mV/s are qualitatively similar to those for the $Pt_{50}Ru_{50}$ alloy:[3] there is a high Tafel slope (ca. 0.5 V/dec) region at low overpotential followed by a transition to a highly active state where the current approaches the diffusion-limiting current; the potential where the transition to the active state occurs decreases with decreasing CO concentration, and the current in the low-overpotential region is roughly inverse half-order in the CO partial pressure (insert, Figure 6). The magnitude of the current in the low-overpotential region is nearly the same on the $Pt_{77}Mo_{23}$ surface versus the $Pt_{50}Ru_{50}$ surface, and about 50 times higher on the alloy surfaces than on the pure Pt surface, but the potential for the transition to the active state on $Pt_{77}Mo_{23}$ occurs at about the same potential as on pure Pt.

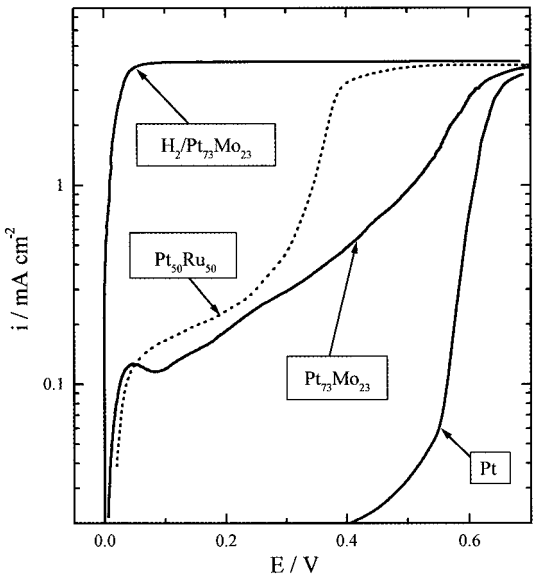

Figure 7. Log i versus potential curves recorded on anodic sweep at 1 mV s^{-1} for oxidation of H_2/0.1% CO on pure Pt, $Pt_{50}Ru_{50}$, and $Pt_{77}Mo_{23}$ surfaces following identical protocols.

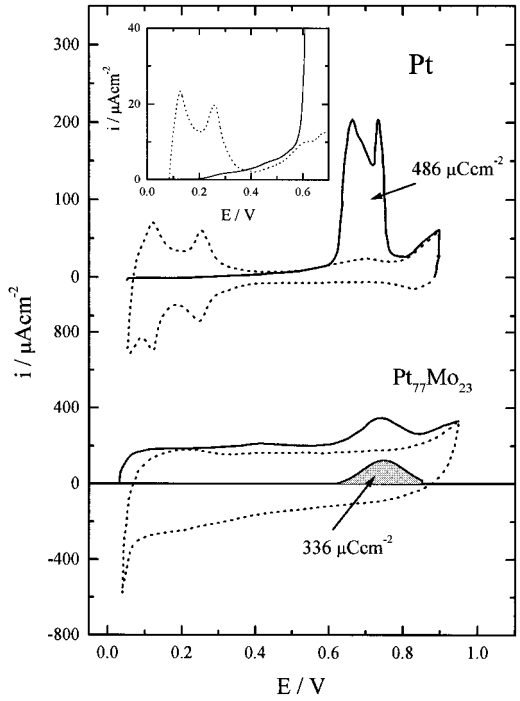

Figure 8. Anodic stripping voltammetry curves for irreversibly adsorbed CO on (upper) Pt and (lower) Pt−Mo alloy. (insert) Expanded current scale for the low potential region on Pt. Dashed curves are recorded after the first anodic sweep. 333 K, 50 mV s^{-1}.

We had shown previously[2,3] that the transition to the highly active state on both Pt and Pt−Ru alloys occurs at the potential where the anodic stripping of adsorbed CO (denoted hereafter as CO_{ads}) starts. The corresponding anodic stripping curve for $Pt_{77}Mo_{23}$ is shown in Figure 8, with a comparison to pure Pt made. In the anodic stripping experiment, CO is adsorbed by holding the potential at 0.05 V in CO-saturated solution for 10 min, followed by purging the solution with argon for 20 min, and then recording the linear sweep voltammetry (LSV) curve. In the case of the pure Pt surface, by using an expanded current scale in the 0.2−0.5 V region (see insert in Figure 8), one can observe a small "prewave" peak, as first reported by Grambow and Bruckenstein,[18] but the amount of charge under this peak

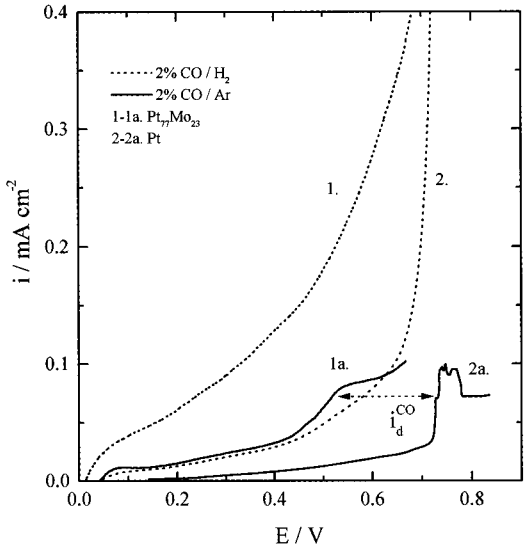

Figure 9. Current−potential curves for (1 and 1a) $Pt_{77}Mo_{23}$ and (2 and 2a) pure Pt for 2% CO in argon and for H2 containing 2% CO recorded with an anodic sweep from 0 V at 1 mV s^{-1}.

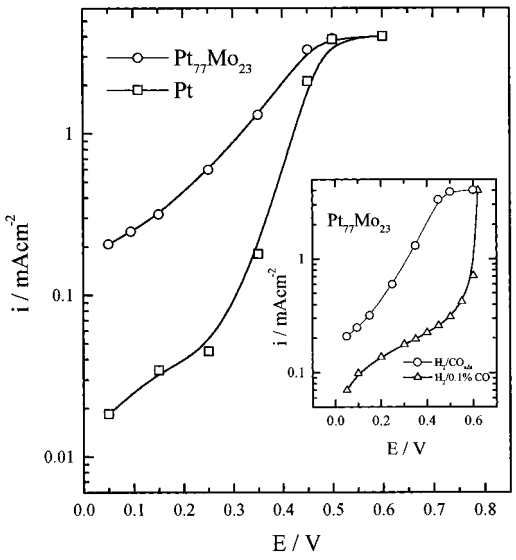

Figure 10. Steady-state currents as a function of potential for H_2 oxidation on $Pt_{77}Mo_{23}$ alloy and pure Pt surfaces with a saturation coverage of CO preadsorbed at 0.05 V. (insert) Comparison of steady-state currents on $Pt_{77}Mo_{23}$ alloy for H_2 oxidation on CO covered surfaces with (Δ) and without (○) 0.1% CO in solution.

is always small, e.g. <10% of the charge under the main stripping peak, and not very reproducible. A detailed discussion of the "prewave" peak can be found in the recent paper by Couto et al.[19] The main CO_{ads} stripping peak for $Pt_{77}Mo_{23}$ is clearly evident in the same potential region as observed for pure Pt, but because of the large pseudocapacitance of the alloy surface in the 0.2−0.6 V region, it is difficult to determine whether some stripping of CO_{ads} occurs in this region as well. We found that the pseudocapacitance near 0.4 V, in particular, cannot be related *entirely* to CO_{ads}, since it is enhanced by holding the potential at 0.05 V even in the absence of CO in solution. There is also an increase in the anodic pseudocapacitance at all potentials after holding the potential at 0.05 V in the absence of CO in solution. This effect means that, for accurate coulometry of the CO_{ads} stripping peak, the LSV curve recorded with the potential hold but without the CO in solution should be used as the "background" current. The resulting stripping current corrected for the pseudocapacitance produces a Pt-like current peak in the 0.6−0.8 V potential region, with an integrated charge of 336 μC cm^{-2}, plus a much smaller amount of charge (25 ± 5 μC cm^{-2}) in the 0.2−0.6 V region that may or may not be CO_{ads} oxidation. If we use the integrated charge from pure Pt as a calibration, with the assumption of one CO per Pt atom in that case, for a 75% Pt surface, one CO per Pt would be a charge of 365 μC cm^{-2}, so a charge of 336 μC cm^{-2} would correspond to a coverage of 0.92 CO per Pt on the alloy surface.

Although we could not obtain definitive evidence that CO_{ads} is being oxidized on the $Pt_{77}Mo_{23}$ surface in the 0.05−0.6 V potential region by LSV, we did observe the continuous oxidation of dissolved CO in this potential region. This result is shown in Figure 9 using 2% CO in argon. The reaction order for CO in this potential region is approximately inverse half-order, so that use of higher concentrations produces such low currents that one is again faced with separating the faradaic current from the capacitive current even using slow sweeping. The use of concentrations lower than 2% results in diffusion-limiting currents (denoted i_d^{CO} in Figure 9) that are so low that they limit the potential region where kinetic information may be obtained. CO (2%) in argon appeared to produce the best results for our purposes here. The potential dependence of the current in the 0.1−0.5 V potential region is the same for H_2 with 2% CO as for 2% CO in argon, the latter being a constant multiple (ca. 4) of the former; this result implies that the oxidation of H_2 is directly coupled to the oxidation of dissolved CO and CO_{ads}. The CO oxidation current on the $Pt_{77}Mo_{23}$ surface in this potential region is ca. 5 times higher than for the pure Pt surface, and we suggest that this is the fundamental reason the activity of the alloy for the oxidation of H_2/CO mixtures is superior to that of pure Pt.

Further support for this interpretation is provided by the results of experiments shown in Figure 10 with both $Pt_{77}Mo_{23}$ and pure Pt surfaces. We call this experiment "the H_2 magnifier" for the way in which it magnifies and illuminates very small changes in CO_{ads} coverage. In this experiment, CO is adsorbed from CO-saturated solution by holding the potential at 0.05 V for 10 min, followed by purging the CO from solution with argon, and then switching to pure H_2 gas. Hydrogen oxidation currents are then recorded potentiostatically after stepping to various potentials; in these experiments, the current reaches a steady-state value relatively quickly, e.g., less than 1 min. These currents represent the oxidation on an electrode surface "poisoned" by preadsorption of CO, but without CO in solution. If CO_{ads} is desorbed or oxidized as the potential increases, in this experiment there is no possibility for readsorption of CO from solution, and thus the surface does not need to "turn over" CO continuously to become "unpoisoned". In the case of the pure Pt surface, there is a very sharp increase in the H_2 oxidation current as the potential is stepped above 0.35 V, which appears to correlate with the oxidation of a small amount of the CO_{ads} in the prewave to the main stripping peak. On $Pt_{77}Mo_{23}$, the current below 0.35 V is about 10 times that on pure Pt and increases steadily with increasing potential, reaching the diffusion-limiting current at about 0.5 V. With reference to Figure 10, note that on both surfaces the current for H_2 oxidation reaches the diffusion-limiting current (at the highest rotation rate used in this work) *below the potential at which the main CO_{ads} stripping peak is observed.* The most reasonable explanation of the data in Figure 10, in our view, is that very small amounts of CO_{ads} are progressively oxidized and/or desorbed on both the $Pt_{77}Mo_{23}$ and the pure Pt surface as the potential is increased from 0.05 to 0.5 V, and the

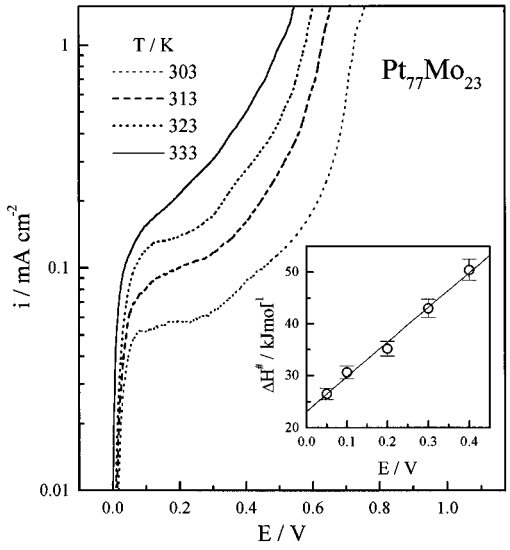

Figure 11. Effect of temperature on the polarization curves for the oxidation of 0.1% CO/H_2 mixture on the $Pt_{77}Mo_{23}$ alloy surface at 1 mV s^{-1}.

corresponding large increase in H_2 oxidation rate is related to a highly nonlinear effect of CO_{ads} on the kinetics. As further evidence of this interpretation, we noted that with the pure Pt surface, after reaching a potential of 0.55 V, the cell was purged with argon and the CO_{ads} stripping curve obtained, producing a CO_{ads} charge about 80% of that for the "fully poisoned surface". In this interpretation, the 10 times higher current at 0.05−0.3 V on $Pt_{77}Mo_{23}$ versus the pure Pt surface is due to a lower coverage by CO_{ads} on the Pt sites of the alloy surface at all potentials in this region. This interpretation is consistent with the difference in saturation coverage at 0.05 V in the anodic stripping experiment described above, e.g., 92% of the coverage on pure Pt.

3.2.3. Oxidation of H_2/CO Mixtures—Temperature Effect. In the course of this investigation, we observed a complex temperature dependence in the oxidation of H_2/CO mixtures on both the $Pt_{77}Mo_{23}$ and the pure Pt surfaces. This is illustrated by the current−potential curves at different temperatures for 0.1% CO/H_2 in Figure 11. The apparent activation energy, defined as the slope of the log I vs T^{-1} curve for constant overpotential, increases monotonically with potential (insert). We are not aware of any previous reports of a potential-dependent activation energy for this reaction. At low overpotential, e.g., 0.05 V, the apparent activation energy is about 10 kJ/mol higher than that for the clean CO-free Pt surface[20] and increases with increasing potential, so that at 0.5 V it approaches the apparent activation energy for the oxidation of dissolved CO on Pt−Ru, ca. 70 kJ/mol.[21] It appears that the activation energy for H_2 oxidation in the presence of CO is a convolution of the activation energies for H_2 and CO oxidation, consistent with the interpretation we have presented above of a coupling of the two reactions even in the potential region below 0.4 V. However, a more substantive analysis of the interesting temperature dependence reported here for the oxidation of the 0.1% CO/H_2 mixture on the $Pt_{77}Mo_{23}$ surface will await a more detailed kinetic modeling effort than we have undertaken in this study.

4. Discussion

Consider a simple site-blocking model[22] for the poisoning of H_2 oxidation by adsorbed CO, given by

$$i_{CO} = i_H(1 - \Theta_{CO})^2 \quad (2)$$

where i_{CO} is the current in the presence of CO either adsorbed on the surface or solution, i_H is the current for pure H_2, and Θ_{CO} is the CO_{ads} coverage, all at a given potential. Let us apply this model first to the H_2 magnification experiments, where the surfaces are poisoned by irreversibly adsorbed CO. At least for the pure Pt surface, we can measure Θ_{CO} independently from the stripping curves in Figure 9 and test the model. For our purposes here, we are interested in testing the model to explain the behavior of electrodes with a high coverage of CO and the effects of small changes in that coverage on H_2 kinetics. To do this in a meaningful way, it must be recognized that there is an inherent problem is determining the absolute CO coverage as the coverage approaches unity, but *changes in coverage* can be measured very accurately by anodic stripping. For a polycrystalline surface, the uncertainty in the experimentally determined CO coverages at saturation as measured by any method known to us, e.g., coulometry or IR spectroscopy, is greater than ±5%. This uncertainty arises from the combination of uncertainty in the determination of the absolute the number of Pt atoms per unit area of electrode surface and the precision in determining the absolute number of CO molecules on the surface. For single-crystal Pt electrodes, where these uncertainties should be minimized, Chang and Weaver[23] have proposed the following absolute values for the saturation coverages: 0.65 CO per Pt for the (111) face, 0.85 for the (100), and 1.0 for the (110) face. However, for a polycrystalline surface, depending on the facets (if any) which constitute the face, the coverage could be anywhere from 0.65 to 1.0, with the additional uncertainty of the surface roughness and CO adsorption at steps and other types of defects. Hence, in our opinion, the integrated charge for our poly Pt electrode of 486 μC/cm^2 could represent any value between 0.9 and 1.0 CO per Pt. However, we can minimize the problem this uncertainty in absolute coverage poses for testing the kinetic model by rewriting the expression, taking advantage of the fact that the change in CO coverage by anodic oxidation can be measured very precisely. The fraction of the CO coverage at saturation, at 0.05 V, that is removed at a more positive potential by oxidation is given by the ratio of q/Q, where q is the CO-stripping charge at the potential of interest, and Q is the total charge to strip all the CO_{ads}. If we let Θ_{CO}° be the saturation coverage at 0.05 V, then the number of free Pt sites, $(1 - \Theta_{CO})$, in the site-blocking model be rewritten as

$$(1 - \Theta_{CO}) = \Theta_{CO}^{\circ}(q/Q) \quad (3)$$

so the kinetic expression may be rewritten as

$$i_{CO} = i_H(1 - \Theta_{CO})^2 = i_H(\Theta_{CO}^{\circ})^2(q/Q)^2 \quad (4)$$

In applying this model to the data, we will make the assumption that in the potential region above 0.20 V, where we will apply the model, the H_2 reaction has no potential dependence other than that produced by the potential-dependent change in Θ_{CO}; i.e., i_H is independent of potential. This is consistent with the assumption made in deriving the site-blocking model,[22] that the reaction follows the Tafel−Volmer mechanism, which reaches a reaction limiting current on Pt above 0.2 V overpotential [ref 21 and references therein]. To test the model for our data for pure Pt, we have plotted in Figure 12 the changes in CO coverage with potential (q) obtained from the anodic stripping curves and the log i_{CO} versus log(q/Q) for the potential region from 0.2 to 0.5 V, the latter having a slope that is very close to

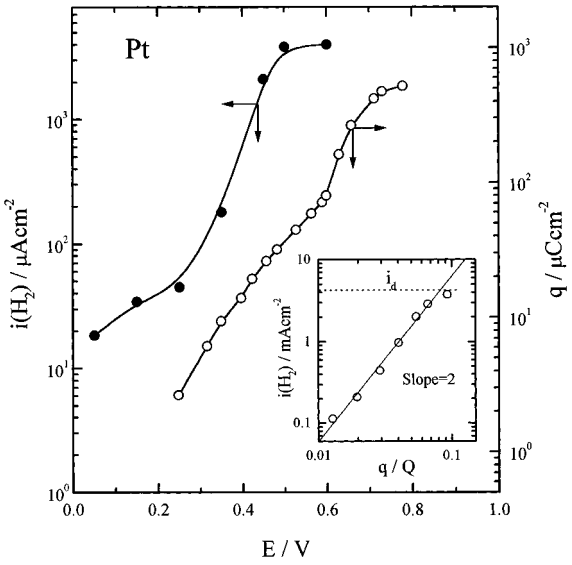

Figure 12. Steady-state currents as a function of potential for H_2 oxidation on a pure Pt surface with a saturation coverage of CO preadsorbed at 0.05 V and the corresponding anodic charges (q) for stripping of the CO remaining on the surface at each potential. (insert) Correlation of the oxidation current with the fraction of the total CO coverage remaining on the surface (q/Q) at 333 K.

2, as predicted by this simple model. Note that removing only 10% of the CO adsorbed at 0.05 V raises the current to the diffusion limiting current at the highest rotation rate we used in this work.

We can then with some reasonableness use this model to rationalize the enhanced activity of the $Pt_{77}Mo_{23}$ surface versus pure Pt. In the case of the $Pt_{77}Mo_{23}$ surface, we have the indication by the same anodic stripping procedure that the coverage by CO_{ads} on the Pt surface atoms of the alloy at 0.05 V is only 92% of that on the pure Pt surface. The magnitude of this reduction in CO coverage on the H_2 oxidation current predicted by the site-blocking model will depend on the value of the absolute coverage; i.e., the value of Θ_{CO}° on the pure Pt surface becomes the scale factor for the effect. Assuming Θ_{CO}° is between 0.95 and 0.98, the model predicts enhancement factors of 6−24, spanning the 10-fold increase actually observed. This simple site-blocking model thus provides at least a working hypothesis concerning the mechanism of action of Mo in the Pt surface in this particular experiment, the hydrogen magnification experiment, which by design illuminates the effect of small changes in CO coverage on H_2 oxidation: Mo appears to reduce the saturation coverage of irreversibly adsorbed CO *on the Pt surface atoms*.

It is more difficult to analyze the data for the oxidation of the H_2/CO mixtures in terms of any kinetic model, since there is in this case additional adsorption of CO from solution, and this amount cannot be easily measured independently. In the context of the present experiments, its presence is seen as additional poisoning of the surface when the CO is present in solution as compared to the analogous experiment with preadsorbed CO, and no CO is in solution. This is shown in the insert in Figure 10 for the $Pt_{77}Mo_{23}$ surface. (A qualitatively similar drop in current occurs for pure Pt, not shown.) The increase in the coverage by adsorbed CO would not have to be much to produce the 3-fold decrease in current density, e.g., from 0.92 to 0.95 CO per Pt in the simple kinetic model we have proposed. In the presence of CO in solution, the steady-state coverage by CO_{ads} is determined by a balance between the rate of adsorption (k_{ad}) and the rate of removal by oxidation (k_{ox}), as represented by the simple series sequence

$$CO(gas) \xrightarrow{k_{ad}} CO_{ads} \xrightarrow{k_{ox}} CO_2 \qquad (5)$$

Both k_{ad} and k_{ox} are potential and temperature dependent, and k_{ad} would also have a CO partial pressure dependence. One could derive a full kinetic model based on eqs 2 and 5, but the number of kinetic parameters is large compared to the limited data set. Conceptually, one can see by the form of eq 5 that the steady-state coverage of CO, Θ_{CO}, which controls the rate of H_2 oxidation via eq 2, is determined by the relative values of k_{ad} and k_{ox}. Suppose, for example, that k_{ox} has a much greater potential dependence than k_{ad}. Then as the potential is increased, one would expect the steady-state value of Θ_{CO} to decrease and the current for H_2 oxidation to increase, and at a potential where Θ_{CO} decreases rapidly with potential, such as at potentials near the CO_{ads} stripping peak, the H_2 current will rise very sharply, just as we see in the experimental curves. Also, this simple expression illustrates another important concept, that the absolute rate of oxidative removal of CO need not be very large if the rate of adsorption is slow, which is a reasonable supposition at the high coverages we are dealing with here.

Gottesfeld and co-workers[24] have recently derived a kinetic model for the oxidation of H_2/CO mixtures on Pt and Pt−Ru catalysts using essentially eqs 2 and 5. Their modeling does demonstrate the validity of the basic concept used in the interpretation of the results in this work: that the continuous oxidation of CO (and CO_{ads}) on the alloy surfaces, e.g., Pt−Ru in the case of[24] or $Pt_{77}Mo_{23}$ in our case here, even at an extremely low rate (e.g., 10 nA/cm^2 [24]), is responsible for the enhancement (vs pure Pt) in the current in the low-potential region of 0.05−0.3 V. According to this model, the qualitatively similar shape of the polarization curves with H_2/CO mixtures for $Pt_{77}Mo_{23}$ and $Pt_{50}Ru_{50}$ alloy surfaces shown in Figure 7 is more than coincidence; the similarity results from an essentially identical mechanism of action of the alloying constituents, Mo and Ru. In view of the very different electrochemistry of these two elements, this is a surprising and nonintuitive conclusion.

Why or how Mo has this effect is unclear. There is spectroscopic evidence that Mo surface atoms have multiple O and/or OH ligands on them at all potentials, and these ligands may be effective in oxidizing adsorbed CO on the neighboring Pt sites, and thus Mo may have the same bifunctional mechanism of action as Ru in the Pt−Ru alloys.[3] Of course, simply having adatoms in the surface with O/OH ligands does not in itself produce activity for CO oxidation. These ligands must be reactive with CO (either dissolved or adsorbed) and rapidly regenerable by extraction from H_2O. An additional mechanism of action could involve the reactivity of the CO_{ads} on the Pt sites as well, perhaps by an electronic interaction between Pt and Mo. It seems likely that some combinations of both of these factors are involved or are even interconnected. Anderson and co-workers[25] made quantum chemical calculations for a bifunctional reaction path (which included all of the foregoing factors) on a Pt surface containing 42 different substitutional alloying elements. These calculations indicated "the early first transition series metals appear especially promising, and the early second transition series are also potentially active in attracting and dissociating H_2O". Mo does fall into the latter category, although it should be noted that both Pt−Ti and Pt−Zr are counterexamples, neither alloy having enhanced activity for the electrooxidation of CO.[26]

5. Summary

The kinetics of H_2 oxidation are not measurably affected by the presence of the Mo in the surface. The shapes of the polarization curves for the oxidation of the H_2/CO mixtures are qualitatively similar to those for the $Pt_{50}Ru_{50}$ alloy examined previously: a high current−potential slope (ca. 0.5 V/dec) at low overpotential followed by a transition to a highly active state where the current approaches the diffusion-limiting current; the potential where the transition to the active state occurs decreases with decreasing CO concentration and decreases with increasing temperature; the current in the low-overpotential region is roughly inverse half-order in the CO partial pressure. The current densities in the low-overpotential region are comparable to those on $Pt_{50}Ru_{50}$ alloy and about a factor of 50 times those on a pure Pt surface. While the anodic stripping of irreversibly adsorbed CO (CO_{ads}) is very different from that on the $Pt_{50}Ru_{50}$ alloy, with most of the CO_{ads} being oxidized only above 0.6 V (RHE), there is direct evidence for the oxidation of small amounts of CO_{ads} in the low-overpotential region of 0.05−0.5 V. The mechanism of action of Mo in the Pt surface in enhancing H_2 oxidation in the presence of CO thus appears to be very similar to that of Ru: a reduction in the steady-state coverage of CO_{ads} by oxidative removal, freeing Pt sites for H_2 oxidation.

Acknowledgment. This work was supported by the Assistant Secretary for Energy Efficiency and Renewable Energy, Office of Transportation Technology, of the U.S. Department of Energy under Contract DE-AC03-76SF00098.

References and Notes

(1) Gasteiger, H.; Markovic, N.; Ross, P. *J. Phys. Chem.* **1995**, *99*, 8945.
(2) Gasteiger, H.; Markovic, N.; Ross, P. *J. Phys. Chem.* **1995**, *99*, 8290.
(3) Gasteiger, H.; Markovic, N.; Ross, P. *J. Phys. Chem.* **1995**, *99*, 16757.
(4) Gasteiger, H.; Markovic, N.; Ross, P. *Catal. Lett.* **1996**, *36*, 1.
(5) Grgur, B.; Zhuang, G.; Markovic, N.; Ross, P. *J. Phys. Chem. B* **1997**, *101*, 3910.
(6) (a)Pearson, W. In *A Handbook of Lattice Spacings and Structures of Metals and Alloys*; Pergammon Press: Oxford, UK, 1958; p 755. (b) Honig, R.; Kramer, D. *RCA Rev.* **1969**, *30*, 285.
(7) Pine Instrument Company, 101 Industrial Drive, Grove City, PA 16127.
(8) Gasteiger, H.; Ross, P.; Cairns, E. *Surf. Sci.* **1993**, *293*, 67.
(9) Markovic, N.; Gasteiger, H.; Ross, P. *J. Phys. Chem.* **1995**, *99*, 3411.
(10) Riviere, J. *Surface Analytical Techniques*; Oxford University Press: Oxford, UK, 1990; p 451.
(11) Baun, W. In *Quantitative Surface Analysis of Materials*; ASTM STP 643; McIntyre, N. S., Ed.; American Society for Testing and Materials: Philadelphia, PA, 1978; p 150.
(12) Mukherjee, S.; Moran-Lopez, J. *Surf. Sci.* **1987**, *189/190*, 1135.
(13) Ross, P. *J. Vac. Sci. Technol. A* **1992**, *10*, 2546.
(14) Miedema, A.; de Chatel, P.; de Boer, F. *Physica B&C* **1980**, *100B*. Miedema, A.; Niessen, A. *Physica B&C* **1982**, *114B*, 367.
(15) Lu, Y.; Clayton, C. *Corros. Sci.* **1989**, *8*, 927.
(16) Derry, G.; Ross, P. *Surf. Sci.* **1984**, *140*, 165.
(17) Koetz, R.; Barbero, C.; Haas, O. *J. Electroanal. Chem.* **1990**, *296*, 37.
(18) Grambow, L.; Bruckenstein, S. *Electrochim. Acta* **1977**, *22*, 377.
(19) Couto, A.; Perez, M.; Rincon, A.; Gutierrez, C. *J. Phys. Chem.* **1996**, *100*, 19538.
(20) Markovic, N.; Grgur, B.; Ross, P. *J. Phys. Chem. B* **1997**, *101*, 5405.
(21) Arico, A.; Modica, E.; Passalacqua, E.; Antonucci, V.; Antonucci, P. *J. Appl. Electrochem.* **1997**, *27*, 1275.
(22) Vogel, W.; Lundquist, J.; Ross, P.; Stonehart, P. *J. Electroanal. Chem.* **1975**, *20*, 79.
(23) Chang, S.-C.; Weaver, M. *J. Phys. Chem.* **1991**, *95*, 5391.
(24) Springer, T.; Zawadzinski, T.; Gottesfeld, S. 192nd Meeting of The Electrochemical Society, Paris France, 1997, to be published in the *Proceedings of the Symposium on "Batteries and Fuel Cells for Portable Applications and Electric Vehicles"*; The Electrochemical Society: Pennington, NJ, 1998.
(25) Anderson, A.; Grantscharova, E.; Seong, S. *J. Electrochem. Soc.* **1996**, *143*, 2075.
(26) Ross, P. In *Electrocatalysis*; Lipkowski, J., Ross, P., Eds.; J. Wiley and Sons: New York, 1998; Chapter 4, in press.